Original Research Communication

Deficiency in mitochondrial complex I activity due to *Ndufs6* gene trap insertion induces renal disease.

Josephine M. Forbes[1,2,3,*], Bi-Xia Ke[4,f*], Tuong-Vi Nguyen[1], Darren C. Henstridge[5], Sally A. Penfold[1], Adrienne Laskowski[4], Karly C. Sourris[1,3], Lukas N. Groschner[1], Mark E. Cooper[1,3], David R. Thorburn[4], Melinda T. Coughlan[1,3]

[1]Glycation and Diabetes Complications Laboratory, Baker IDI Heart & Diabetes Institute, Melbourne, Victoria, 8008, Australia.

[2]Glycation and Diabetes, Mater Medical Research Institute, South Brisbane, Queensland, 4101, Australia.

[3]Departments of Medicine and Immunology, Monash University, Alfred Medical Research & Education Precinct, Melbourne, 3004, Victoria, Australia

[4]Murdoch Children's Research Institute, Royal Children's Hospital and Department of Paediatrics, University of Melbourne, Parkville 3052, Victoria, Australia.

[5]Cellular and Molecular Metabolism Laboratory, Baker IDI Heart & Diabetes Institute, Melbourne 8008, Victoria, Australia.

*These authors contributed equally to this work

Corresponding Author:

Melinda Coughlan

Diabetes Complications Laboratory

Baker IDI Heart & Diabetes Institute

PO Box 6492, St Kilda Rd Central, Melbourne, 8008, Australia.

Telephone: +61 3 8532 1278, Fax: +61 3 8532 1480

Email: Melinda.Coughlan@bakeridi.edu.au

Running title: Complex I deficiency and kidney disease

Word count: 6056

Number of references: 69

Number of greyscale illustrations: 3

Number of color illustrations: 3

Abstract

Aims: Defects in the activity of enzyme complexes of the mitochondrial respiratory chain are thought to be responsible for several disorders including renal impairment. Gene mutations which result in complex I deficiency are the most common OXPHOS disorders in humans. To determine if an abnormality in mitochondrial complex I *per se* is associated with development of renal disease, mice with a knockdown of the complex I gene, *Ndufs6* were studied.

Results: *Ndufs6* mice had a partial renal cortical complex I deficiency; *Ndufs6*$^{gt/gt}$, 32% activity and *Ndufs6*$^{gt/+}$, 83% activity compared to WT mice. Both *Ndufs6*$^{gt/+}$ and *Ndufs6*$^{gt/gt}$ mice exhibited hallmarks of renal disease including albuminuria, urinary excretion of kidney injury molecule-1 (Kim-1), renal fibrosis and changes in glomerular volume, with decreased capacity to generate mitochondrial ATP and superoxide from substrates oxidised via complex I. However, more advanced renal defects in *Ndufs6*$^{gt/gt}$ mice were observed in the context of a disruption in the inner mitochondrial electrochemical potential, 3-nitrotyrosine-modified mitochondrial proteins, increased urinary excretion of 15-isoprostane F_{2t} and upregulation of antioxidant defence. Juvenile *Ndufs6*$^{gt/gt}$ mice also exhibited signs of early renal impairment with increased urinary Kim-1 excretion and elevated circulating cystatin C.

Innovation: We have identified renal impairment in a mouse model of partial complex I deficiency, suggesting that even modest deficits in mitochondrial respiratory chain function may act as risk factors for chronic kidney disease.

Conclusion: These studies identify for the first time that complex I deficiency as the result of interruption of *Ndufs6* is an independent cause of renal impairment.

Introduction

The incidence of chronic kidney disease is a growing health concern in developed nations[1], particularly in light of recent studies that have identified renal dysfunction as a major predictor of all-cause mortality[34]. Chronic kidney disease is classically defined as a decline in blood filtration by units termed the glomeruli within the kidney cortex, in the presence of leakage of protein into the urine or structural abnormalities. Complex I (NADH:ubiquinone oxidoreductase), the largest complex of the mitochondrial respiratory chain, is comprised of at least 45 unique subunits including NADH dehydrogenase (ubiquinone) iron-sulfur protein 6 (Ndufs6), which is a highly conserved subunit[17]. Complex I is an entry point for electrons into the respiratory chain and mediates a large majority of cellular energy production by the transfer of electrons in the process of oxidative phosphorylation (OXPHOS)[24]. This highly efficient process involves the generation of an electrochemical gradient as protons are pumped across the inner mitochondrial membrane, supporting the synthesis of ATP[24]. Complex I is also a major contributor to reactive oxygen species (ROS) production in the cell under certain conditions[37].

Abnormalities in OXPHOS are observed at an incidence of approximately 1 in 5000 births[54]. Of these, mutations that result in deficiencies in complex I are the most commonly seen in humans[27,61] and these manifest with a broad range of clinically relevant presentations including neurodegeneration, heart failure and significant mortality in childhood and adolescence. A number of studies have shown that renal disease can result from deficiencies in OXPHOS as a result of mutations in Coenzyme Q_{10} biosynthesis monooxygenase 6[23], *Pdss2*[38], cytochrome c oxidase 10[64], p53-controlled ribonucleotide reductase[4] and cytochrome b[11] in humans and

animal models. However, there is no previous study directly linking mutations in specific complex I subunits to chronic renal disease.

Previous reports have shown genetic mutations resulting in no expression of *NDUFS6,* the second most conserved subunit of complex I, to be fatal in humans[26,56]. We generated a unique mouse model using gene-trap technology which, to our surprise, was not embryonic lethal, but due to tissue specific splicing, had a partial knockdown of *Ndufs6* expression in various tissues including the kidney (approximately 10% mRNA expression[25]). In this model, the kidney has 32% deficiency in Complex I activity in homozygous *Ndufs6*$^{gt/gt}$ mice. Since approximately half of all patients with Complex I deficiency show substantial variation in Complex I activity between tissues, this mouse provides a relevant model system for studying renal dysfunction. We have identified that this loss of function via interruption of *Ndufs6* expression results in a renal disease phenotype.

Results

Generation of Complex I deficient mice

Ndufs6$^{gt/gt}$ mice were generated by knockdown of the Ndufs6 gene using gene-trap embryonic stem cell lines as previously described[25]. *Ndufs6*$^{gt/gt}$ mice had a partial knockdown of the *Ndufs6* gene, with small amounts of wild-type (WT) mRNA detected in all tissues studied[25]. In the kidney, *Ndufs6* mRNA expression, measured by quantitative real time PCR, was 55±7% of WT mRNA in heterozygous *Ndufs6*$^{gt/+}$ mice (n=6 per group) and 11±1% of WT mRNA in homozygous *Ndufs6*$^{gt/gt}$ mice (n=8 per group; Mean±SEM).

WT mice had 550±122 mU complex I activity per U citrate synthase (CS) activity in renal cortices (mean±SD). There was less activity of complex I in renal cortices from both heterozygous gene-trap mice (*Ndufs6*$^{gt/+}$, 456±135 mU/U; 83% of WT; $P<0.05$ vs WT) and in homozygous gene-trap mice (*Ndufs6*$^{gt/gt}$, 175±25 mU/U; 32% of WT, $P<0.01$ vs WT, $P<0.05$ vs *Ndufs6*$^{gt/+}$). CS activity was greater in mice with complex I deficiency compared to WT (WT, 250.2±94.1 nmol/min/mg; *Ndufs6*$^{gt/+}$, 400.1±59.1 nmol/min/mg $P<0.05$; *Ndufs6*$^{gt/gt}$, 471.4±95.3 nmol/min/mg $P<0.001$; Mean±SD).

Complex I deficiency did not alter body weight (WT, 38.6±8.4 g; *Ndufs6*$^{gt/+}$, 41.1±10.1 g; *Ndufs6*$^{gt/gt}$, 38.7±8.0 g; Mean±SD), kidney weight-to-body-weight ratio (WT, 11.1±0.4x10^{-3}; *Ndufs6*$^{gt/+}$, 12.0±2.3 x10^{-3}; *Ndufs6*$^{gt/gt}$, 10.6±2.2 x10^{-3} Mean±SD), or heart weight-to-body-weight ratio (WT, 6.1±1.5x10^{-3}; *Ndufs6*$^{gt/+}$, 6.3±1.1x10^{-3}; *Ndufs6*$^{gt/gt}$, 12.5±8.3 x10^{-3}; Mean±SD).

Complex I deficiency disrupts ATP production in the kidney

Isolated renal cortical mitochondria from *Ndufs6*$^{gt/gt}$ and *Ndufs6*$^{gt/+}$ mice showed decreased capacity to generate ATP from substrates oxidised via complex I (glutamate and malate, Figure 1A), but not via complex II (succinate in the presence of the complex I inhibitor rotenone, Figure 1B). The mitochondrial transmembrane potential ($\Delta\psi_m$) was decreased in isolated renal cortical mitochondria from *Ndufs6*$^{gt/gt}$ mice (Figure 1C), similar to that observed with the chemical uncoupler carbonylcyanide-m-chlorophenylhydrazone (CCCP). A tendency of $\Delta\psi_m$ to decrease was observed in mitochondria from heterozygotes (*Ndufs6*$^{gt/+}$ mice), however this failed to reach significance.

Mitochondrial reactive oxygen species and antioxidant defence

Mitochondria are a significant source of ROS, which are increasingly considered to play a key role in renal pathology[6,12,15,28]. In addition, complex I is a site of electron leakage, with subsequent generation of superoxide and hydrogen peroxide[37]. Thus, we measured ROS generation by mitochondria in renal cortices. In the presence of complex I-linked substrates (glutamate plus malate), superoxide production was decreased in both *Ndufs6*$^{gt/gt}$ and *Ndufs6*$^{gt/+}$ mice compared to WT mice (Figure 2A representative flow cytometry histograms and Figure 2B quantitation). A similar result was obtained in the presence of substrates for complex II (succinate and rotenone), in which superoxide production decreased in *Ndufs6*$^{gt/gt}$ and *Ndufs6*$^{gt/+}$mice compared to WT mice (Figure 2C and D).

In the presence of complex I substrates (glutamate plus malate) hydrogen peroxide generation was increased in isolated renal mitochondria from mice with complex I deficiency (Figure 2E). When complex II-linked substrates were provided, hydrogen peroxide decreased (Figure 2F) in *Ndufs6*$^{gt/+}$ and *Ndufs6*$^{gt/gt}$ mice.

MnSOD (SOD2) is essential for superoxide detoxification within mitochondria[16]. Upregulation in the activity of MnSOD activity was observed in isolated mitochondria from mice homozygous for complex I gene deletion (*Ndufs6*$^{gt/gt}$; Figure 3A), which was not apparent in heterozygotes (*Ndufs6*$^{gt/+}$) mice. In addition, the mitochondrial content of 3-nitrotyrosine, a stable marker of peroxynitrite production, was also increased in *Ndufs6*$^{gt/gt}$ mice, indicative of more pronounced ROS production with greater loss of complex I activity (Figure 3B). Similarly, an increase in urinary 15-isoprostane F_{2t} excretion, a marker of lipid peroxidation, was apparent in complex I deficient mice, which was increased to a greater extent in *Ndufs6*$^{gt/gt}$ mice (Figure 3C).

Complex I deficient mice have abnormal renal function and morphology

Urinary albumin-to-creatinine ratio (ACR) was increased in both *Ndufs6*$^{gt/+}$ and *Ndufs6*$^{gt/gt}$ mice (Figure 4A), indicative of impaired renal function. Shedding of kidney injury molecule-1 (Kim-1) into the urine, an early biomarker of renal tubular dysfunction[21,63] was apparent in both *Ndufs6*$^{gt/+}$ and *Ndufs6*$^{gt/gt}$ mice (Figure 4B). Renal structural changes were evident in mice with complex I deficiency, with abnormal deposition of renal cortical collagen in the extracellular matrix, reminiscent of progressive renal disease, observed in both *Ndufs6*$^{gt/+}$ and *Ndufs6*$^{gt/gt}$ mice (Figure 4C). Representative photomicrographs of renal cortical collagen accumulation which is indicated by light blue staining, are shown, in WT (Figure 4 top panel), *Ndufs6*$^{gt/+}$ (Figure 4 middle panel) and *Ndufs6*$^{gt/gt}$ (Figure 4 bottom panel). Tubulointerstitial area remained unchanged (Figure 4D), whilst activation of the profibrotic cytokine transforming growth factor (TGF)-β1 (Figure 4E), in the renal cortex was observed in mice with complex I deficiency.

Further histologic examination revealed some damaged glomerular microvascular beds in both *Ndufs6*$^{gt/+}$ and *Ndufs6*$^{gt/gt}$ mice, reflected by an increase in glomerulosclerosis following staining using the Periodic Acid Schiff method (Pictured in Figure 5, WT top panel, *Ndufs6*$^{gt/+}$ middle panel and *Ndufs6*$^{gt/gt}$ bottom panel and quantified in Figure 5A). Notably, homozygous *Ndufs6* mice had a greater degree of glomerulosclerosis compared to heterozygotes.

Upon further investigation of renal cortical architecture, loss of function of complex I led to glomerular hypertrophy demonstrated by increased glomerular volume (Figure 5B). Moreover, there was an increase in hyperplasia present within glomerular cross-sections (Figure 5C), which incrementally associated with the decline in activity of complex I, with homozygous *Ndufs6*$^{gt/gt}$ mice having the greatest number of glomerular cells present.

Mild renal impairment is present in Ndufs6$^{gt/gt}$ mice early in life

Our previous study showed that Ndufs6$^{gt/gt}$ mice developed cardiac abnormalities as early as one month of life[25]. In order to ascertain if renal impairment was likely to precede cardiac abnormalities, WT, *Ndufs6*$^{gt/+}$ and *Ndufs6*$^{gt/gt}$ mice were studied at 16 days of life (n=5 per group). There was no difference observed in ACR (Figure 6A) or plasma creatinine (Figure 6B). However, a more sensitive marker of glomerular filtration, cystatin C, was increased in the circulation of *Ndufs6*$^{gt/gt}$ mice, in parallel with urinary excretion of Kim-1 (Figure 6D). Urinary 15-isoprostane F_{2t} excretion was unchanged (Figure 6E), and there was no evidence of glomerulosclerosis (Figure 6F).

Discussion

In this study we utilized a mouse model generated using gene-trap technology to disrupt the gene expression of the complex I subunit *Ndufs6*, to investigate a direct causative role of partial complex I deficiency in the development of renal disease. In heterozygotes (*Ndufs6*$^{gt/+}$ mice), complex I activity in renal cortex was 83% of that in WT mice. Homozygous mice (*Ndufs6*$^{gt/gt}$ mice) had only 32% complex I activity compared to WT. Data obtained in this study indicate that even a partial renal deficiency in the activity of complex I, as observed in *Ndufs6*$^{gt/+}$ mice, was sufficient to manifest significant renal disease, although there was some evidence of more advanced glomerular injury in homozygous mice, which had the greatest impairment of complex I activity. This is the first time that specific decline in the activity of complex I of the mitochondrial respiratory chain has been shown to induce renal impairment.

There is some precedent for abnormalities in OXPHOS as a result of genetic mutations contributing to renal impairment in humans[48]. The most common manifestation is de Toni-Debre-Fanconi syndrome[46,66]. Genetic defects in complex III assembly[11], complex IV[64], mitochondrial DNA[47,58] and coenzyme Q10[23] have been associated with a renal phenotype in the context of deficiency in the activity of other electron transport chain complexes. In an experimental model of chronic kidney disease, diabetic nephropathy, we have previously demonstrated a deficiency in complex I activity[10], in addition to therapeutic benefits of coenzyme Q10[55].

In the present study, both *Ndufs6*$^{gt/+}$ and *Ndufs6*$^{gt/gt}$ mice exhibited hallmarks of chronic kidney disease. Urinary ACR and Kim-1 were increased compared to WT mice, in parallel with renal cortical collagen deposition and fibrosis indicated by active TGF-β1 and damaged microvascular beds of the glomeruli. These functional

and structural changes occurred in the context of different activity levels of complex I inherent to genotype. Homozygous *Ndufs6*$^{gt/gt}$ mice post-500 days of age displayed greater damage to the glomerulus when compared heterozygotes. Indeed, juvenile homozygous mice studied at day 16 of age already had evidence of tubular damage, as indicated by accelerated Kim-1 excretion and changes in glomerular filtration as measured by cystatin C.

Mitochondrial respiratory chain defects that result in renal pathology in humans show a variety of lesions within the kidney including tubular casts and atrophy, dilatation and tubulointerstititial fibrosis as previously reviewed[48]. Prior evidence indicates that tubular dysfunction is a prominent manifestation resulting from mitochondrial abnormalities in the kidney, as shown by studies exploring diseases such as de Toni-Debre-Fanconi syndrome[33], drug related toxicity[19] and infection[8]. Indeed in the present study, early tubular dysfunction was demonstrated, as reflected by an increase in shedding of Kim-1 into the urine[21,63] from both *Ndufs6*$^{gt/+}$ and *Ndufs6*$^{gt/gt}$ mice. Although fibrosis specific to the tubulointerstitium was not assessed, total cortical fibrosis, as measured by an increase in cortical collagen deposition in association with activation of TGF-β1 was evident in mice with complex I deficiency and was associated with renal functional defects.

As is often observed in human mitochondriopathies, complex I deficiency in *Ndufs6*$^{gt/gt}$ kidneys resulted in an impaired capacity to generate ATP from substrates oxidised via complex I. This occurred in both homozygous and heterozygous mice and was dependent on Complex I activity, as ATP production from complex-II-linked substrates was unchanged. These data indicate that even a nominal loss of biochemical function of Complex I (such as in heterozygotes, 83% of wild type) within the kidney confers a significant defect, which disrupts oxidative

phosphorylation. There are several explanations for comparable ATP synthesis in heterozygotes and homozygotes. It is possible that the more severe renal damage in homozygous mice resulted in alterations in cellular composition of the kidney, with different cell types explaining the apparent differences in Complex I activity thresholds. Indeed, the glomeruli from homozygous mice exhibited hyperplasia, which is indicative of changes in cell type. Though this phenomenon was not observed in the heterozygous mice. A more likely explanation is the sensitivity of the kidney to changes in oxidative phosphorylation, in particular from glucose-derived substrates due to a high proportion of proximal tubules (almost 90%) within the renal cortex[42]. Unlike the cells of the glomerulus, proximal tubule epithelial cells rely on aerobic respiration for ATP synthesis, having a limited glycolytic capacity[2,22]. The high ATP requirement in proximal tubules is necessary for active transport across concentration gradients that occur during the reabsorption of glucose, peptides and other macromolecules from the glomerular filtrate to prevent urinary losses.

In keeping with the glomerular podocyte as a possible site of mitochondrial dysfunction and subsequent renal injury, some patients with respiratory chain disorders exhibit glomerular disease with nephrotic syndrome, characterised by larger glomerular volume and cellular hyperplasia[20,33]. Moreover, an eloquent study that explored the renal phenotype of the *Pdss2* mutant mouse model[31,38], which results in a biosynthetic defect in mitochondrial Coenzyme Q and subsequent electron transport chain impairment, demonstrated that nephritis originated specifically within the glomerular podocyte, as renal disease was apparent in *Podocin/cre,Pdss2*$^{loxP/loxP}$ knockout mice, but not in conditional knockouts targeted to the renal tubular epithelium[38]. It is possible that both sites are equally important in disease pathogenesis in the *Ndufs6* mouse model, since glomerular fibrosis and

hypertrophy were also observed in *Ndufs6*$^{gt/+}$ and *Ndufs6*$^{gt/gt}$ mice. It is interesting however, that more advanced glomerular injury was evident with lower complex I activity, which leads us to speculate that cells of the glomerulus are less susceptible to injury unless there is substantial complex I deficiency, as was seen in homozygous mice within the present study. One limitation of our study is the lack of blood pressure monitoring. We cannot rule out haemodynamic changes within the renal cortex as a contributor to the renal phenotype observed in Ndufs6 mutant mice. Further studies are needed to elucidate the cellular localization of the primary defect.

Our data suggests that a specific decrease in Ndufs6 expression, resulting in a partial deficiency in the activity of complex I, negatively impacts mitochondrial respiratory chain function. Mitochondria obtained from kidney cortices of mice with knockdown of *Ndufs6* expression resulting in complex I deficiency demonstrated functional abnormalities. Mitochondrial changes associated with the more severe renal phenotype observed in homozygous *Ndufs6* mice included loss of mitochondrial membrane potential and upregulation of the key mitochondrial antioxidant MnSOD. Biomarkers of ROS-induced damage that were also apparent in homozygous *Ndufs6* mice included mitochondrial 3-nitrotyrosine, formed upon nitration of protein tyrosine residues with the reactive nitrogen species peroxynitrite or nitrogen dioxide[14], and urinary excretion of 15-isoprostane F_{2t}, a chemically stable end-product of lipid peroxidation derived from arachidonic acid[43]. 15-isoprostane F_{2t} is considered a sensitive and specific indicator of oxidative stress status[44] and was measured to ascertain if an increased oxidative stress status was secondary to the decline in mitochondrial respiratory chain function.

Within the mitochondria, it is plausible that the decline in respiratory chain function may have precipitated electron leakage at complex I, with subsequent

superoxide radical formation[39], which, upon reaction with nitric oxide, mediated formation of peroxynitrite, which is known to alter electron transport[40]. Indeed, there was a decrease in renal mitochondrial generation of superoxide and an excess formation of hydrogen peroxide in the presence of complex I-linked substrates. Since MnSOD activity was also upregulated or unchanged in *Ndufs6*$^{gt/gt}$ and *Ndufs6*$^{gt/+}$ mice respectively, the decrease in superoxide may be interpreted as a result of rapid conversion of superoxide anion to hydrogen peroxide by MnSOD, in addition to rapid binding of superoxide to nitric oxide forming peroxynitrite, since the accumulation of 3-nitrotyrosine was observed.

Hydrogen peroxide, which was increased in both genotypes, can be rapidly converted to damaging hydroxyl radicals, though this was not determined within the current study. Perhaps as equally important, hydrogen peroxide can serve as a second messenger, facilitating the induction of the redox-sensitive transcription factor nuclear factor-κB[52] with subsequent chemokine upregulation, triggering infiltration of inflammatory cells within the peritubular and glomerular compartments. The inflamed microenvironment can stimulate fibrogenic cytokine production that drives cell dedifferentiation and epithelial-to-mesenchymal transition[30,67] and tubular atrophy. Not surprisingly, ROS have been suggested to exacerbate chronic kidney disease[10,15].

A common manifestation of mitochondrial respiratory chain disorders in patients is cardiomyopathy[29,68]. In a recent study, we have shown that homozygous Ndufs6$^{gt/gt}$ mice developed cardiomyopathy and in some instances cardiac failure and death by approximately 300 days of life[25]. This was associated with severe impairment of complex I activity in the heart as a consequence of almost no wild type RNA for *Ndufs6* at this tissue site. It should be noted that in that study, Ndufs6$^{gt/gt}$

mice surviving beyond day 300 had some cardiac abnormalities, which were absent in heterozygotes. This is in contrast to the current investigation in which renal impairment was observed in both Ndufs6$^{gt/gt}$ and Ndufs6$^{gt/+}$ mice, which each had an impaired expression of wild type mRNA in the kidney[25] leading to renal deficiency in the activity of complex I. Furthermore, we demonstrated that juvenile homozygous Ndufs6$^{gt/gt}$ mice, less than 16 days of life, already had some evidence of early renal impairment which precedes cardiac defects which are evident from day 21 of life. This may suggest that cardiomyopathy and renal disease each have a different pathogenesis following complex I deficiency. Indeed, the heart and kidney differ in fuel utilization for energy production, with the heart preferring free fatty acids and the kidney consuming glucose-derived molecules. Since in the current study, mice were specifically selected that survived long term (post 500 days), it is likely that we have excluded those mice that manifest more severe consequences of mitochondriopathy. Indeed, no evidence of cardiac hypertrophy was observed in homozygous Ndufs6 mice which were followed in the present study. Therefore it is unlikely that cardiac abnormalities were responsible for the renal disease apparent in the heterozygous mice and in the 16 day old mice. Indeed, renal disease is known to be a major risk factor for cardiovascular disease[51]. In addition, the contribution of the tissue-specific splicing codes[3] may also be responsible for the phenotype exhibited in our mice, suggesting that tissue specific manifestations of complex I deficiency may influence the type of syndrome identified in patients with OXPHOS defects. It is unlikely that tissue-specific splicing contributes to the phenotype in humans with *NDUFS6* mutations since all patients described appear to have had knockout mutations expressed in all tissues studied, resulting in a total loss of complex I activity and early death[26,56]. Rather, it may be that specific cellular insults, such as that seen in

diabetes[10], which lower complex I activity, may impair renal function and result in structural abnormalities. Indeed, this warrants further investigation in other models of chronic kidney disease.

Male mice were selected for this study as there is gender dimorphism of chronic renal disease progression with females significantly protected against renal disease development[50,53]. Although not fully explained, it is considered that functional and structural parameters of the kidney are influenced by interactions of sex hormones with their cognate receptors in the kidney[18,53]. The gender dimorphism of CKD progression may consist of effects of the interaction of circulating androgens and estrogens with specific kidney receptors[50]. Indeed, 17β-estradiol inhibits inflammatory and pro-apoptotic processes and protects kidney function in aging rats[32].

Complex I is composed of 45 different subunits[7], which must be assembled correctly for proper function. In the current mouse model, decreased amounts of the Ndufs6 subunit result in decreased amounts of assembled Complex I[25]. Other Complex I subunits are typically unstable and degrade if not incorporated into a stable complex[35]. Therefore we cannot rule out that changes in other complex I proteins may have contributed to the renal phenotype observed within our study.

A caveat to our study is the limitations that exist using probes such as MitoSox Red and hydroethidine to measure intracellular superoxide production with detection by fluorescence (extensively reviewed in[69]). Albeit our study has assessed substrate-induced superoxide production in isolated mitochondria, thus avoiding the issues associated with intracellular uptake and distribution, kinetics and availability of the probe[69]. Nevertheless, the superoxide data generated within the current study should be interpreted with caution due to the possible confounding effects of the

nonspecific oxidation product(s) of MitoSox Red contributing to the total fluorescence intensity. HPLC separation of hydroethidium oxidation products with electrochemical detection provides selective detection of 2-hydroxyethidium, the product of the reaction of MitoSox Red/hydroethidine and superoxide, and therefore is a more specific method of analysing superoxide production[69].

Taken together, our study indicates a causative role for deficiency of complex I of the mitochondrial respiratory chain in the development of kidney disease, specifically via mutations of *Ndufs6*. The renal phenotype appeared to be independent of cardiomyopathy, since (i) there was no evidence of cardiac hypertrophy, (ii) kidney disease was evident in *Ndufs6*$^{gt/+}$ which have not been reported to have significant cardiac abnormalities[25], and, (iii) an early decline in renal function was exhibited by Ndufs6$^{gt/gt}$ mice at 16 days of life, which was prior to the onset of cardiomyopathy. These data suggest that mutations resulting in a partial deficiency in the activity of complex I of the mitochondrial respiratory chain within the kidney may be worth considering as an initiator of chronic renal disease.

Innovation

Mitochondrial complex I deficiency is the most common mitochondrial enzyme defect in humans. Several mitochondriopathies have been associated with renal impairment, however the effects of complex I deficiency on the development of chronic kidney disease *per se* is not known. In this study we have identified that kidney disease is induced in a novel mouse model with gene-trap *Ndufs6* knockdown that exhibits a partial deficiency in complex I with concomitant disruption in renal mitochondrial function. Our study suggests that even modest deficits in complex I activity may act as a significant risk factor for chronic kidney disease.

Materials and Methods

Ndufs6 Gene Trap Mouse model

Mice with a knockdown of the *Ndufs6* gene were generated using gene-trap embryonic stem cell lines, as described elsewhere[25]. These mice have a vector insertion in intron 2 of the *Ndufs6* gene, that generates a fusion protein that cannot be incorporated into the multi-subunit NADH:ubiquinone oxidoreductase (complex I) of the electron transport chain within mitochondria[25]. However, some tissues retain up to 35% of normal levels of wild-type Ndufs6 mRNA, due to tissue-specific splicing over the vector, allowing some wild type mRNA and protein to be formed.

Male homozygous (*Ndufs6*$^{gt/gt}$), heterozygous (*Ndufs6*$^{gt/+}$) and WT mice (WT; 75% C57BL/6J/25% 129/O1a background), n=8 mice per group, were selected that survived in excess of 500 days (509±57, 527±29 or 523±31 days respectively) in order to explore the development of renal disease over lifespan. Mice that lost more than 20% body weight were excluded from the study. Animals were housed in groups of five mice per cage with a 12 h light/dark cycle and *ad libitum* access to food and water. At the completion of the study, spot urine samples were collected, mice were killed and kidneys were either snap frozen in liquid nitrogen and stored at -80°C, formalin fixed, or used immediately for mitochondrial isolation and subsequent functional assays as described below. All animal experiments were performed in accordance with guidelines from the Murdoch Children's Research Institute Animal Ethics Committee and the National Health and Medical Research Council of Australia.

Renal Functional Analysis

Urinary ACR was used as a marker of renal function. Urinary albumin was determined by sandwich ELISA (Bethyl Laboratories, Montgomery, TX, USA) as

previously described[59]. Creatinine in urine was determined by HPLC (Agilent HP1100 system, Hewlett Packard, Boblingen, Germany) as previously described[59]. All urinary parameters were standardized to urinary creatinine. Urinary content of Kim-1 (USCN Life Sciences, Wuhan, China), considered a sensitive marker of tubular injury[62], was measured using a commercially available sandwich ELISA according to the manufacturer's instructions.

Histological assessment of renal injury

The extent of renal injury was assessed by morphometric analysis of the glomerulus and tubular interstitium. Mouse renal cortices were fixed in 10% neutral buffered formalin, embedded in paraffin, deparaffinized in xylene, then sections were stained with hematoxylin and eosin, periodic acid Schiff (PAS), or Masson's trichrome. Glomerulosclerotic index (GSI) was assessed in 3-μm paraffin embedded Periodic Acid Schiff (PAS) stained sections by a semi-quantitative method as previously described[49]. Briefly, sections were examined using an Olympus CH20 light microscope (Tokyo, Japan) at a magnification of x400. Thirty glomeruli within each kidney were randomly selected and graded according to the severity of the glomerular damage: 0, normal; 1, minimal glomerular damage, the mesangial matrix and/or hyalinosis with focal adhesion, involving <25% of the glomerulus; 2, moderate sclerosis of 26 to 50%; 3, moderate-severe sclerosis of 51 to 75%; 4, severe sclerosis of >75% of the glomerulus. The GSI was calculated by using the following formula:

$$GSI = (1 \times n_1) + (2 \times n_2) + (3 \times n_3) + (4 \times n_4)/n_0 + n_1 + n_2 + n_3 + n_4$$

where n_x = number of glomeruli in each grade of glomerulosclerosis. This analysis was performed with the observer blinded to the treatment groups.

The volume of glomeruli in the outer cortex of each kidney was determined in haemotoxylin and eosin stained sections (4 μm) using the point-counting method described by Weibel and Gomez[65]. Glomerular volume was measured in 20 glomeruli per mouse using Image-Pro Plus software (Media Cybernetics, MD, USA). In addition, the number of glomerular nuclei for 20 glomeruli randomly selected across one histological section was counted.

Total cortical collagen was assessed in twenty fields (x100) of Masson's Trichrome stained kidney sections (4 μm) using Image-Pro Plus.

Tubulointerstitial area was evaluated in PAS-stained sections by point counting technique using a 1 cm^2 eyepiece graticule with 9 equidistant grid lines. Ten randomly selected corticomedullary areas per mouse were evaluated and 81 grid intersection points per field were counted at 200x magnification. The percentage fractional area was calculated as follows:

%FA= (number of tubulointerstitial grid intersections/total number of grid intersections) x 100

TGF-β1 ELISA

TGF-β1 is a profibrotic cytokine, known to play an important role in fibrosis in chronic kidney disease[5]. Renal cortices were fractionated as previously described[59]. Biologically active TGF-β1 was measured in plasma membrane fractions using the TGF-β1 Emax ImmunoAssay System (Promega, Madison, WI) according to the manufacturer's instructions. Prior to measurement, samples were diluted 1 in 5 with PBS, then acid activated with 5-10 μl 1 M HCl to a pH of approximately 3.0. After a 15 min incubation at room temperature, samples were neutralized with approximately 5.0 μl 1 M NaOH to achieve a pH of approximately 7.6. Samples were then used within the immunoassay without further dilution. Values were expressed

as pg/mg of protein as determined by the bicinchoninic acid method (Pierce, Rockford, IL, USA).

Mitochondrial isolation

Mitochondria were isolated by differential centrifugation. Freshly harvested renal cortex (100 mg) was finely minced and gently homogenized with glass teflon tissue grinders in 4 ml ice-cold isolation medium, pH 7.4 (250 mM sucrose, 10 mM Tris-HCl, 1 mM EGTA). The homogenate was centrifuged at 720 *g* for 5 min at 4°C and the resulting supernatant was centrifuged at 15,300 *g* for 10 min at 4°C. After washing, the mitochondrial pellet was resuspended in 300 μl ice-cold respiration medium (225 mM Mannitol, 75 mM Sucrose, 10 mM Tris-HCl, 10 mM KH_2PO_4, 10 mM KCl, 0.1 mM EDTA, 0.8 mM $MgCl_2$). Total protein was determined by the Bicinchoninic acid method according to the manufacturer's instructions (Pierce, Rockford, IL, USA).

Citrate Synthase activity

Mitochondrial CS activity was performed according to the method of Srere et al.,[57] which employs the measurement of CS activity by linking the release of Coenzyme A to the colorimetric agent DTNB 5,5-dithiobis-2-nitrobenzoate (Ellman's reagent). Mitochondria (15 mg/ml), permeabilized by three freeze-thaw cycles, were diluted 1 in 20 (5 μl mitochondria in 95 μl of 100 mM TRIS buffer pH 8.3). Ten μl of diluted mitochondria, or blank (Tris Buffer pH 8.3) was added to a 96-well microtiter plate (Sarstedt, Nümbrecht, Germany) in duplicate. A reaction mixture was prepared containing 1 mM DTNB, 3 mM Acetyl CoA, and 10% Triton-X in Tris Buffer pH 8.3. Twenty μl of a 7.5 mM oxaloacetate solution was added to 225 μl reaction mixture and the absorbance was measured at 412 nm each minute for 5 min with a BioRad Benchmark Microtitre plate reader. The change in absorbance per minute was

calculated within the linear range of the plot. After correction for the blank, CS activity was calculated using the molar extinction coefficient of TNB at 412 nm of 13.6 mM^{-1} cm^{-1} and a path length of 0.552 cm, and was standardised per renal cortical wet weight.

Mitochondrial superoxide production by flow cytometry

Superoxide production in freshly isolated mitochondria was measured using the MitoSOX Red probe (Molecular Probes, Invitrogen, Eugene, OR, USA) and fluorescence was detected by flow cytometry as previously described[36] but with modifications as described below. MitoSOX Red is hydroethidine coupled to a mitochondrial targeting lipophilic cation triphenylphosphine[45]. With one unpaired electron, the $O_2^{\bullet-}$ radical selectively oxidizes the nonfluorescent hydroethidine moiety to form the fluorescent product 2-hydroxyethidium. This increase in fluorescence is used as an index of relative mitochondrial $O_2^{\bullet-}$ production. MitoSOX Red is readily oxidized by superoxide but not by other ROS- or reactive nitrogen species (RNS)–generating systems. Briefly, 5 μM MitoSOX red was added to 15 μg of mitochondrial protein in 500 μl Hanks Balanced Salt Solution (HBSS, with sodium bicarbonate, calcium and magnesium, without phenol red, pH 7.3) in the presence of either, complex I substrates 10 mM glutamate/10 mM malate, or the complex II substrate 10 mM succinate plus 2.5 μM rotenone. For signal specificity, a positive control containing 0.5 mM hypoxanthine (HX) + 100 mU/ml xanthine oxidase (XO) and a negative control containing 0.5 mM HX + 100 mU/ml XO + 100 U/ml superoxide dismutase was included. HX+XO resulted in an increase in fluorescence intensity compared to PBS control, which was dampened with addition of SOD, indicating specificity of superoxide detection via this method (data not shown). Samples were incubated for 30 min at 37°C in the dark, washed with PBS and analysed on a FACS

Calibur (BD, USA) flow cytometer, using excitation at 400 nm with detection at 590 nm in the FL2 channel. A minimum of 15,000 events per sample were acquired. The data were presented by histograms representing the mean intensity of MitoSOX fluorescence.

Hydrogen peroxide production

Hydrogen peroxide production in renal cortical mitochondrial preparations was measured by fluorescence using the Amplex Red reagent (Molecular Probes, Invitrogen, Melbourne, Australia) as previously described[10]. In addition, hydrogen peroxide production was assessed in the presence of 10 mM glutamate and 10 mM malate or 10 mM succinate plus 2.5 μM rotenone.

ATP production

Mitochondria were isolated by differential centrifugation as described above. ATP production was measured in triplicate using a bioluminescence ATP determination Kit (Molecular Probes, Invitrogen, Melbourne, Australia) as described previously[13] with the following modifications. The complex I substrates, 10 mM glutamate plus 10 mM malate or the Complex II substrate 10 mM succinate plus 2.5 μM rotenone were added to the mitochondrial suspensions (15 μg/well). Luminescence was recorded every 5 seconds for a total analysis time of 30 seconds, with the steady state rate used to determine the rate of ATP production. The ATP production (nmol/min/mg protein) was normalized to CS activity to minimize the effects of variability from altered mitochondrial numbers[41].

Mitochondrial membrane potential

Mitochondrial membrane potential was assessed using the MitoProbe JC-1 assay kit (Molecular Probes) by flow cytometry. Briefly, freshly isolated mitochondria

(50 μg protein) were incubated with 2 μM JC-1 at 37°C for 15 min. A negative (in the absence of JC-1) and positive control (25 μM CCCP) was also added. Suspensions were washed, pelleted, and resuspended in PBS before analysis by flow cytometry (minimum 10,000 events/sample; FACSCalibur; BD Biosciences, San Jose, CA). The ratio of red to green fluorescence intensity was determined.

Superoxide dismutase activity

The activity of superoxide dismutase in isolated mitochondria was measured using a commercially available kit (Cayman Chemical Company, Ann Arbor, MI, USA) as previously described[9].

Complex I activity

Respiratory chain complex I and the mitochondrial marker enzyme CS were assayed in glomerular post-600 *g* supernatants and in hypotonically treated mesangial cell mitochondrial preparations as previously described for other tissues[41], except that the assay temperature was 25°C. To account for variations in mitochondrial number between samples, complex I activity was expressed relative to CS in mU/U. CS is much more resistant to oxidative inactivation than the respiratory chain complexes[60].

15-isoprostane F_{2t} ELISA

Urinary isoprostane excretion (15-isoprostane F_{2t}) was measured by a competitive ELISA specifically designed for urine (Oxford Biomedical Research, Oxford MI), according to the manufacturer's instructions.

3-Nitrotyrosine ELISA

The mitochondrial content of 3-Nitrotyrosine was measured using the Bioxytech Nitrotyrosine EIA kit (Oxis Research, Portland, OR, USA), as specified by the manufacturer.

RNA Isolation and Quantitative PCR Analysis.

RNA isolation and quantitative PCR was performed as previously described[25]. Briefly, total RNA, isolated from kidney using Illustra RNA Spin mini kit (GE Healthcare), was treated with DNaseI using an Ambion Turbo DNA freeTM kit. cDNA was synthesized using TaqMan reverse transcription reagents (Applied Biosystems) and real-time PCR was performed using TaqMan assays. The signal was detected by Biorad iQ 5 Multicolor real-time PCR detection system. Primers and probes for *Ndufs6* were designed with Primerexpress software (Applied Biosystems) with the probe spanning across the exon 2/3 boundary. Primers and probes for *Gapdh* were purchased from Applied Biosystems. Samples were run in triplicate for both *Ndufs6* and *Gapdh* as the internal control.

Statistics

All statistical computations were performed using GraphPad Prism version 4.0a for Mac OS X (GraphPad Software, San Diego, California, USA). Values of experimental groups are given as mean, with bars showing the SEM, unless otherwise stated. One-way ANOVA with Tukey's post-test analysis was used to determine statistical significance. Where appropriate, a two-tailed t-test was performed. A $p < 0.05$ was considered to be statistically significant.

Acknowledgments

The authors would like to thank Amy Morley, Vicki Thallas-Bonke, Brooke Harcourt, Edward Grixti and Maryann Arnstein for their technical expertise. This work was completed with support from the Juvenile Diabetes Research Foundation (JDRF), the National Health and Medical Research Council of Australia (NHMRC) and the Victorian Government's Operational Infrastructure Support Program. Melinda Coughlan holds a Skip Martin Australian Diabetes Society Early Career Fellowship. Josephine Forbes is an NHMRC Research Fellow. Darren Henstridge is supported by a Postdoctoral Fellowship from The National Heart Foundation of Australia. David Thorburn is an NHMRC Principal Research Fellow. Mark Cooper is an NHMRC Australia Fellow as well as a JDRF scholar.

Author Disclosure Statement

No competing financial interests exist

List of Abbreviations

Albumin to creatinine ratio (ACR)

Carbonylcyanide-m-chlorophenylhydrazone (CCCP)

Citrate synthase (CS)

Kidney injury molecule-1 (Kim-1)

Manganese superoxide dismutase (MnSOD)

NADH dehydrogenase (ubiquinone) iron-sulfur protein 6 (Ndufs6*)*

Oxidative phosphorylation (OXPHOS)

Reactive oxygen species (ROS)

Transforming growth factor (TGF)

Wild type (WT)

References

1. Bakris GL, Ritz E. The message for World Kidney Day 2009: hypertension and kidney disease: a marriage that should be prevented. Kidney Int 2009;75(5):449-52.
2. Balaban RS, Mandel LJ. Metabolic substrate utilization by rabbit proximal tubule. An NADH fluorescence study. Am J Physiol 1988;254(3 Pt 2):F407-16.
3. Barash Y, Calarco JA, Gao W, Pan Q, Wang X, Shai O, Blencowe BJ, Frey BJ. Deciphering the splicing code. Nature 2010;465(7294):53-9.
4. Bourdon A, Minai L, Serre V, Jais JP, Sarzi E, Aubert S, Chretien D, de Lonlay P, Paquis-Flucklinger V, Arakawa H and others. Mutation of RRM2B, encoding p53-controlled ribonucleotide reductase (p53R2), causes severe mitochondrial DNA depletion. Nat Genet 2007;39(6):776-80.
5. Brosius FC, 3rd. New insights into the mechanisms of fibrosis and sclerosis in diabetic nephropathy. Rev Endocr Metab Disord 2008;9(4):245-54.
6. Cachofeiro V, Goicochea M, de Vinuesa SG, Oubina P, Lahera V, Luno J. Oxidative stress and inflammation, a link between chronic kidney disease and cardiovascular disease. Kidney Int Suppl 2008(111):S4-9.
7. Carroll J, Fearnley IM, Skehel JM, Shannon RJ, Hirst J, Walker JE. Bovine complex I is a complex of 45 different subunits. J Biol Chem 2006;281(43):32724-7.
8. Conaldi PG, Biancone L, Bottelli A, Wade-Evans A, Racusen LC, Boccellino M, Orlandi V, Serra C, Camussi G, Toniolo A. HIV-1 kills renal tubular epithelial cells in vitro by triggering an apoptotic pathway involving caspase activation and Fas upregulation. J Clin Invest 1998;102(12):2041-9.
9. Coughlan MT, Thallas-Bonke V, Pete J, Long DM, Gasser A, Tong DC, Arnstein M, Thorpe SR, Cooper ME, Forbes JM. Combination therapy with the advanced glycation end product cross-link breaker, alagebrium, and angiotensin converting enzyme inhibitors in diabetes: synergy or redundancy? Endocrinology 2007;148(2):886-95.
10. Coughlan MT, Thorburn DR, Penfold SA, Laskowski A, Harcourt BE, Sourris KC, Tan AL, Fukami K, Thallas-Bonke V, Nawroth PP and others. RAGE-induced cytosolic ROS promote mitochondrial superoxide generation in diabetes. J Am Soc Nephrol 2009;20(4):742-52.
11. de Lonlay P, Valnot I, Barrientos A, Gorbatyuk M, Tzagoloff A, Taanman JW, Benayoun E, Chretien D, Kadhom N, Lombes A and others. A mutant mitochondrial respiratory chain assembly protein causes complex III deficiency in patients with tubulopathy, encephalopathy and liver failure. Nat Genet 2001;29(1):57-60.
12. Del Vecchio L, Locatelli F, Carini M. What we know about oxidative stress in patients with chronic kidney disease on dialysis--clinical effects, potential treatment, and prevention. Semin Dial 2011;24(1):56-64.
13. Drew B, Leeuwenburgh C. Method for measuring ATP production in isolated mitochondria: ATP production in brain and liver mitochondria of Fischer-344 rats with age and caloric restriction. Am J Physiol Regul Integr Comp Physiol 2003;285(5):R1259-67.
14. Feeney MB, Schoneich C. Tyrosine modifications in aging. Antioxid Redox Signal 2012;17(11):1571-9.
15. Forbes JM, Coughlan MT, Cooper ME. Oxidative stress as a major culprit in kidney disease in diabetes. Diabetes 2008;57(6):1446-54.

16. Fukai T, Ushio-Fukai M. Superoxide dismutases: role in redox signaling, vascular function, and diseases. Antioxid Redox Signal 2011;15(6):1583-606.
17. Gabaldon T, Rainey D, Huynen MA. Tracing the evolution of a large protein complex in the eukaryotes, NADH:ubiquinone oxidoreductase (Complex I). J Mol Biol 2005;348(4):857-70.
18. Grzegorczyk K, Krajewska M, Weyde W, Jakuszko K, Gniewek A, Klinger M. [Gender and kidney diseases: the clinical importance and mechanisms of modifying effects]. Postepy Hig Med Dosw (Online) 2011;65:849-57.
19. Hall AM, Unwin RJ. The not so 'mighty chondrion': emergence of renal diseases due to mitochondrial dysfunction. Nephron Physiol 2007;105(1):p1-10.
20. Hall AM, Unwin RJ, Hanna MG, Duchen MR. Renal function and mitochondrial cytopathy (MC): more questions than answers? QJM 2008;101(10):755-66.
21. Han WK, Bailly V, Abichandani R, Thadhani R, Bonventre JV. Kidney Injury Molecule-1 (KIM-1): a novel biomarker for human renal proximal tubule injury. Kidney Int 2002;62(1):237-44.
22. Harris SI, Balaban RS, Barrett L, Mandel LJ. Mitochondrial respiratory capacity and Na+- and K+-dependent adenosine triphosphatase-mediated ion transport in the intact renal cell. J Biol Chem 1981;256(20):10319-28.
23. Heeringa SF, Chernin G, Chaki M, Zhou W, Sloan AJ, Ji Z, Xie LX, Salviati L, Hurd TW, Vega-Warner V and others. COQ6 mutations in human patients produce nephrotic syndrome with sensorineural deafness. J Clin Invest 2011;121(5):2013-24.
24. Hirst J. Towards the molecular mechanism of respiratory complex I. Biochem J 2010;425(2):327-39.
25. Ke BX, Pepe S, Grubb DR, Komen JC, Laskowski A, Rodda FA, Hardman BM, Pitt JJ, Ryan MT, Lazarou M and others. Tissue-specific splicing of an Ndufs6 gene-trap insertion generates a mitochondrial complex I deficiency-specific cardiomyopathy. Proc Natl Acad Sci U S A 2012;109(16):6165-70.
26. Kirby DM, Salemi R, Sugiana C, Ohtake A, Parry L, Bell KM, Kirk EP, Boneh A, Taylor RW, Dahl HH and others. NDUFS6 mutations are a novel cause of lethal neonatal mitochondrial complex I deficiency. J Clin Invest 2004;114(6):837-45.
27. Koopman WJ, Nijtmans LG, Dieteren CE, Roestenberg P, Valsecchi F, Smeitink JA, Willems PH. Mammalian mitochondrial complex I: biogenesis, regulation, and reactive oxygen species generation. Antioxid Redox Signal 2010;12(12):1431-70.
28. Libetta C, Sepe V, Esposito P, Galli F, Dal Canton A. Oxidative stress and inflammation: Implications in uremia and hemodialysis. Clin Biochem 2011;44(14-15):1189-98.
29. Limongelli G, Tome-Esteban M, Dejthevaporn C, Rahman S, Hanna MG, Elliott PM. Prevalence and natural history of heart disease in adults with primary mitochondrial respiratory chain disease. Eur J Heart Fail 2010;12(2):114-21.
30. Lopez-Novoa JM, Nieto MA. Inflammation and EMT: an alliance towards organ fibrosis and cancer progression. EMBO Mol Med 2009;1(6-7):303-14.
31. Lyon MF, Hulse EV. An inherited kidney disease of mice resembling human nephronophthisis. J Med Genet 1971;8(1):41-8.

32. Maric C, Sandberg K, Hinojosa-Laborde C. Glomerulosclerosis and tubulointerstitial fibrosis are attenuated with 17beta-estradiol in the aging Dahl salt sensitive rat. J Am Soc Nephrol 2004;15(6):1546-56.
33. Martin-Hernandez E, Garcia-Silva MT, Vara J, Campos Y, Cabello A, Muley R, Del Hoyo P, Martin MA, Arenas J. Renal pathology in children with mitochondrial diseases. Pediatr Nephrol 2005;20(9):1299-305.
34. Matsushita K, van der Velde M, Astor BC, Woodward M, Levey AS, de Jong PE, Coresh J, Gansevoort RT. Association of estimated glomerular filtration rate and albuminuria with all-cause and cardiovascular mortality in general population cohorts: a collaborative meta-analysis. Lancet 2010;375(9731):2073-81.
35. Mimaki M, Wang X, McKenzie M, Thorburn DR, Ryan MT. Understanding mitochondrial complex I assembly in health and disease. Biochim Biophys Acta 2012;1817(6):851-62.
36. Mukhopadhyay P, Rajesh M, Yoshihiro K, Hasko G, Pacher P. Simple quantitative detection of mitochondrial superoxide production in live cells. Biochem Biophys Res Commun 2007;358(1):203-8.
37. Murphy MP. How mitochondria produce reactive oxygen species. Biochem J 2009;417(1):1-13.
38. Peng M, Falk MJ, Haase VH, King R, Polyak E, Selak M, Yudkoff M, Hancock WW, Meade R, Saiki R and others. Primary coenzyme Q deficiency in Pdss2 mutant mice causes isolated renal disease. PLoS Genet 2008;4(4):e1000061.
39. Pitkanen S, Robinson BH. Mitochondrial complex I deficiency leads to increased production of superoxide radicals and induction of superoxide dismutase. J Clin Invest 1996;98(2):345-51.
40. Radi R, Rodriguez M, Castro L, Telleri R. Inhibition of mitochondrial electron transport by peroxynitrite. Arch Biochem Biophys 1994;308(1):89-95.
41. Rahman S, Blok RB, Dahl HH, Danks DM, Kirby DM, Chow CW, Christodoulou J, Thorburn DR. Leigh syndrome: clinical features and biochemical and DNA abnormalities. Ann Neurol 1996;39(3):343-51.
42. Rebelo L, Carmo-Fonseca M, Moura TF. Redistribution of microvilli and membrane enzymes in isolated rat proximal tubule cells. Biol Cell 1992;74(2):203-9.
43. Roberts LJ, 2nd, Morrow JD. The generation and actions of isoprostanes. Biochim Biophys Acta 1997;1345(2):121-35.
44. Roberts LJ, Morrow JD. Measurement of F(2)-isoprostanes as an index of oxidative stress in vivo. Free Radic Biol Med 2000;28(4):505-13.
45. Ross MF, Kelso GF, Blaikie FH, James AM, Cocheme HM, Filipovska A, Da Ros T, Hurd TR, Smith RA, Murphy MP. Lipophilic triphenylphosphonium cations as tools in mitochondrial bioenergetics and free radical biology. Biochemistry (Mosc) 2005;70(2):222-30.
46. Rotig A. Renal disease and mitochondrial genetics. J Nephrol 2003;16(2):286-92.
47. Rotig A, Goutieres F, Niaudet P, Rustin P, Chretien D, Guest G, Mikol J, Gubler MC, Munnich A. Deletion of mitochondrial DNA in patient with chronic tubulointerstitial nephritis. J Pediatr 1995;126(4):597-601.
48. Rotig A, Munnich A. Genetic features of mitochondrial respiratory chain disorders. J Am Soc Nephrol 2003;14(12):2995-3007.

49. Saito T, Sumithran E, Glasgow EF, Atkins RC. The enhancement of aminonucleoside nephrosis by the co-administration of protamine. Kidney Int 1987;32(5):691-9.
50. Sandberg K. Mechanisms underlying sex differences in progressive renal disease. Gend Med 2008;5(1):10-23.
51. Sarnak MJ, Levey AS, Schoolwerth AC, Coresh J, Culleton B, Hamm LL, McCullough PA, Kasiske BL, Kelepouris E, Klag MJ and others. Kidney disease as a risk factor for development of cardiovascular disease: a statement from the American Heart Association Councils on Kidney in Cardiovascular Disease, High Blood Pressure Research, Clinical Cardiology, and Epidemiology and Prevention. Circulation 2003;108(17):2154-69.
52. Sen CK, Packer L. Antioxidant and redox regulation of gene transcription. FASEB J 1996;10(7):709-20.
53. Silbiger S, Neugarten J. Gender and human chronic renal disease. Gend Med 2008;5 Suppl A:S3-S10.
54. Skladal D, Halliday J, Thorburn DR. Minimum birth prevalence of mitochondrial respiratory chain disorders in children. Brain 2003;126(Pt 8):1905-12.
55. Sourris KC, Harcourt BE, Tang PH, Morley AL, Huynh K, Penfold SA, Coughlan MT, Cooper ME, Nguyen TV, Ritchie RH and others. Ubiquinone (coenzyme Q10) prevents renal mitochondrial dysfunction in an experimental model of type 2 diabetes. Free Radic Biol Med 2012;52(3):716-23.
56. Spiegel R, Shaag A, Mandel H, Reich D, Penyakov M, Hujeirat Y, Saada A, Elpeleg O, Shalev SA. Mutated NDUFS6 is the cause of fatal neonatal lactic acidemia in Caucasus Jews. Eur J Hum Genet 2009;17(9):1200-3.
57. Srere PA. Citrate Synthase (EC4.1.3.7). In: Lowenstein JM, editor. Methods in Enzymology Volume 13. Academic press, New York; 1969. p 3-10.
58. Szabolcs MJ, Seigle R, Shanske S, Bonilla E, DiMauro S, D'Agati V. Mitochondrial DNA deletion: a cause of chronic tubulointerstitial nephropathy. Kidney Int 1994;45(5):1388-96.
59. Tan AL, Sourris KC, Harcourt BE, Thallas-Bonke V, Penfold S, Andrikopoulos S, Thomas MC, O'Brien RC, Bierhaus A, Cooper ME and others. Disparate effects on renal and oxidative parameters following RAGE deletion, AGE accumulation inhibition, or dietary AGE control in experimental diabetic nephropathy. Am J Physiol Renal Physiol 2010;298(3):F763-70.
60. Thorburn DR, Chow CW, Kirby DM. Respiratory chain enzyme analysis in muscle and liver. Mitochondrion 2004;4(5-6):363-75.
61. Tucker EJ, Compton AG, Calvo SE, Thorburn DR. The molecular basis of human complex I deficiency. IUBMB Life 2011;63(9):669-77.
62. Vaidya VS, Ozer JS, Dieterle F, Collings FB, Ramirez V, Troth S, Muniappa N, Thudium D, Gerhold D, Holder DJ and others. Kidney injury molecule-1 outperforms traditional biomarkers of kidney injury in preclinical biomarker qualification studies. Nat Biotechnol 2010;28(5):478-85.
63. Vaidya VS, Ramirez V, Ichimura T, Bobadilla NA, Bonventre JV. Urinary kidney injury molecule-1: a sensitive quantitative biomarker for early detection of kidney tubular injury. Am J Physiol Renal Physiol 2006;290(2):F517-29.
64. Valnot I, von Kleist-Retzow JC, Barrientos A, Gorbatyuk M, Taanman JW, Mehaye B, Rustin P, Tzagoloff A, Munnich A, Rotig A. A mutation in the human heme A:farnesyltransferase gene (COX10) causes cytochrome c oxidase deficiency. Hum Mol Genet 2000;9(8):1245-9.

65. Weibel ER, Gomez DM. A principle for counting tissue structures on random sections. J Appl Physiol 1962;17:343-8.
66. Wendel U, Ruitenbeek W, Bentlage HA, Sengers RC, Trijbels JM. Neonatal De Toni-Debre-Fanconi syndrome due to a defect in complex III of the respiratory chain. Eur J Pediatr 1995;154(11):915-8.
67. Wu Y, Deng J, Rychahou PG, Qiu S, Evers BM, Zhou BP. Stabilization of snail by NF-kappaB is required for inflammation-induced cell migration and invasion. Cancer Cell 2009;15(5):416-28.
68. Yaplito-Lee J, Weintraub R, Jamsen K, Chow CW, Thorburn DR, Boneh A. Cardiac manifestations in oxidative phosphorylation disorders of childhood. J Pediatr 2007;150(4):407-11.
69. Zielonka J, Kalyanaraman B. Hydroethidine- and MitoSOX-derived red fluorescence is not a reliable indicator of intracellular superoxide formation: another inconvenient truth. Free Radic Biol Med 2010;48(8):983-1001.

Figure Legends

Figure 1: Renal mitochondrial functional parameters. ATP production in renal cortical mitochondria isolated from WT, *Ndufs6*$^{gt/+}$mice and *Ndufs6*$^{gt/gt}$ mice and incubated with **(A)** complex I-linked substrates 10 mM glutamate and 10 mM malate, or **(B)** complex II-linked substrates 10 mM succinate and the complex I inhibitor rotenone (2.5 μM). **(C)** Mitochondrial membrane potential ($\Delta\psi$) using the potentiometric dye JC-1 with analysis by flow cytometry. WT wild type, +/- *Ndufs6*$^{gt/+}$mice, -/- *Ndufs6*$^{gt/gt}$ mice. *p <0.05 vs WT mice; #p <0.05 vs Ndufs6$^{+/-}$ mice; n=5-8 per group.

Figure 2: Renal mitochondrial reactive oxygen species generation. Renal cortical mitochondria from WT, *Ndufs6*$^{gt/+}$mice and *Ndufs6*$^{gt/gt}$ mice were assayed for superoxide production using the MitoSox Red dye in the presence of **A-B** 10 mM glutamate and 10 mM malate, or **C-D** 10 mM succinate and 2.5 μM rotenone. Samples were analysed by flow cytometry using excitation at 400 nm with detection at 590 nm in the FL2 channel. Representative histograms showing mean intensity of MitoSOX fluorescence are shown for glutamate/malate (A), and succinate/rotenone (C), with corresponding quantitation shown in B and D respectively. Renal cortical mitochondria were incubated with **(E)** glutamate/malate or **(F)** succinate and rotenone and H_2O_2 production was assessed using the Amplex red assay probe with fluorescence detection. WT wild type, +/- *Ndufs6*$^{gt/+}$mice, -/- *Ndufs6*$^{gt/gt}$ mice. *p <0.05 vs WT mice, n=6-8 per group; n=5 per group.

Figure 3: Manganese Superoxide Dismutase (MnSOD) activity and biomarkers of peroxynitrite damage and lipid peroxidation. Renal mitochondrial **(A)** MnSOD activity as measured by spectrophotometry, and **(B)** 3-nitrotyrosine content measured by enzyme-linked immunosorbent assay (ELISA). **(C)** Urinary 15-isoprostane F_{2t} excretion as measured by ELISA. WT wild type, +/- *Ndufs6*$^{gt/+}$mice, -/- *Ndufs6*$^{gt/gt}$ mice. *p <0.05 vs WT mice; #p <0.05 vs Ndufs6$^{+/-}$ mice; n=8 per group.

Figure 4: Renal phenotype.

(A) Urinary albumin to creatinine ratio (ACR) (data are geomean plus tolerance factor), **(B)** Urinary excretion of Kim-1, **(C)** Quantitation of total cortical collagen determined using Image ProPlus and representative photomicrographs of Masson's trichrome-stained sections of renal cortex from WT mice (top panel), Ndufs6$^{+/-}$ mice (middle panel) and Ndufs6$^{-/-}$ (bottom panel) mice showing collagen deposition in blue (x400 magnification, scale bar is equal to 25 μm). **(D)** Tubulointerstitial area evaluated by point counting technique. **(E)** Active TGF-β1 in renal cortical plasma membrane. WT wild type, +/- *Ndufs6*$^{gt/+}$mice, -/- *Ndufs6*$^{gt/gt}$ mice. *p <0.05 vs WT mice; #p <0.05 vs Ndufs6$^{+/-}$ mice; n=8 per group.

Figure 5: Glomerular injury. Representative photomicrographs of Periodic Acid Schiff (PAS) stained renal sections (x400 magnification, scale bar is equal to 25 μm) from WT mice (top panel), Ndufs6$^{+/-}$ mice (middle panel) and Ndufs6$^{-/-}$ mice (bottom panel), with **(A)** corresponding semiquantitative analysis of glomerulosclerosis. **(B)** Glomerular volume and **(C)** Cells/per glomerulus were assessed histologically as described in materials and methods. WT wild type, +/- *Ndufs6*$^{gt/+}$mice, -/- *Ndufs6*$^{gt/gt}$ mice. *p <0.05 vs WT mice; #p <0.05 vs Ndufs6$^{+/-}$ mice; n=8 per group.

Figure 6: Renal phenotype of juvenile mice.

Urine, plasma and renal cortices were collected from 16 day old wild type, *Ndufs6*$^{gt/+}$ and *Ndufs6*$^{gt/gt}$ mice and renal phenotype was determined. **(A)** Urinary albumin to creatinine ratio (ACR) (data are geomean plus tolerance factor), **(B)** Plasma creatinine as measured by high performance liquid chromatography, **(C)** Plasma cystatin C as measured by enzyme-linked immunosorbent assay (ELISA), **(D)** Urinary excretion of Kim-1 as determined by ELISA, **(E)** Urinary 15-isoprostane F_{2t} excretion as measured by ELISA and **(F)** Semiquantitative analysis of glomerulosclerosis. WT wild type, +/- *Ndufs6*$^{gt/+}$mice, -/- *Ndufs6*$^{gt/gt}$ mice. *p <0.05 vs WT mice; #p <0.05 vs Ndufs6$^{+/-}$ mice; n=3-5 mice per group.

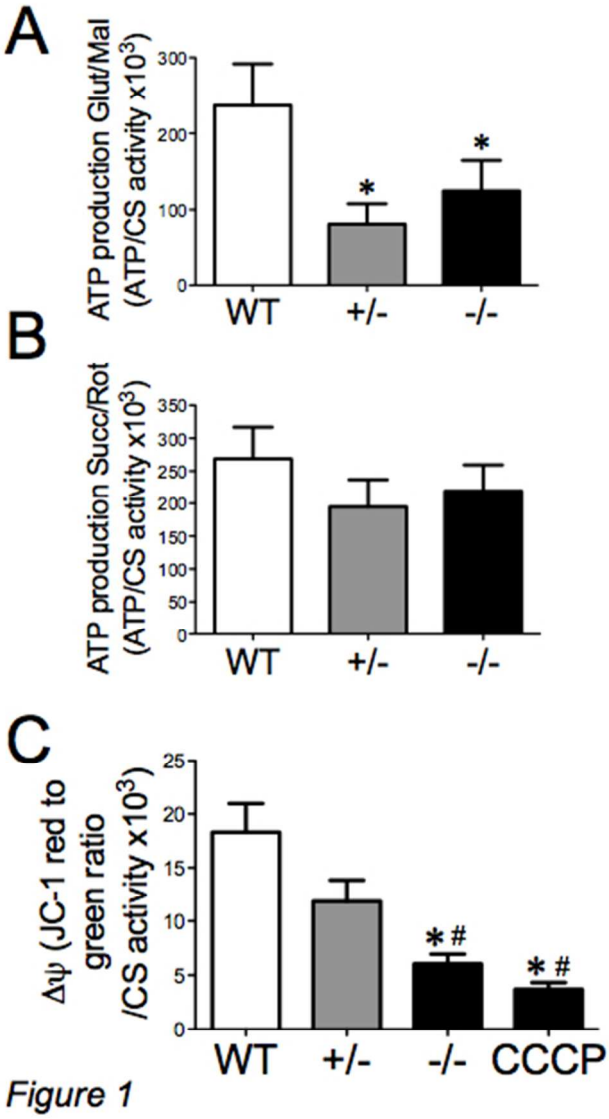

Figure 1

Figure 1: Renal mitochondrial functional parameters. ATP production in renal cortical mitochondria isolated from WT, Ndufs6gt/+mice and Ndufs6gt/gt mice and incubated with (A) complex I-linked substrates 10mM glutamate and 10mM malate, or (B) complex II-linked substrates 10mM succinate and the complex I inhibitor rotenone (2.5μM). (C) Mitochondrial membrane potential (Δψ) using the potentiometric dye JC-1 with analysis by flow cytometry. WT wild type, +/- Ndufs6gt/+mice, -/- Ndufs6gt/gt mice. *p<0.05 vs WT mice; #p<0.05 vs Ndufs6+/- mice; n=5-8 per group.
108x170mm (100 x 100 DPI)

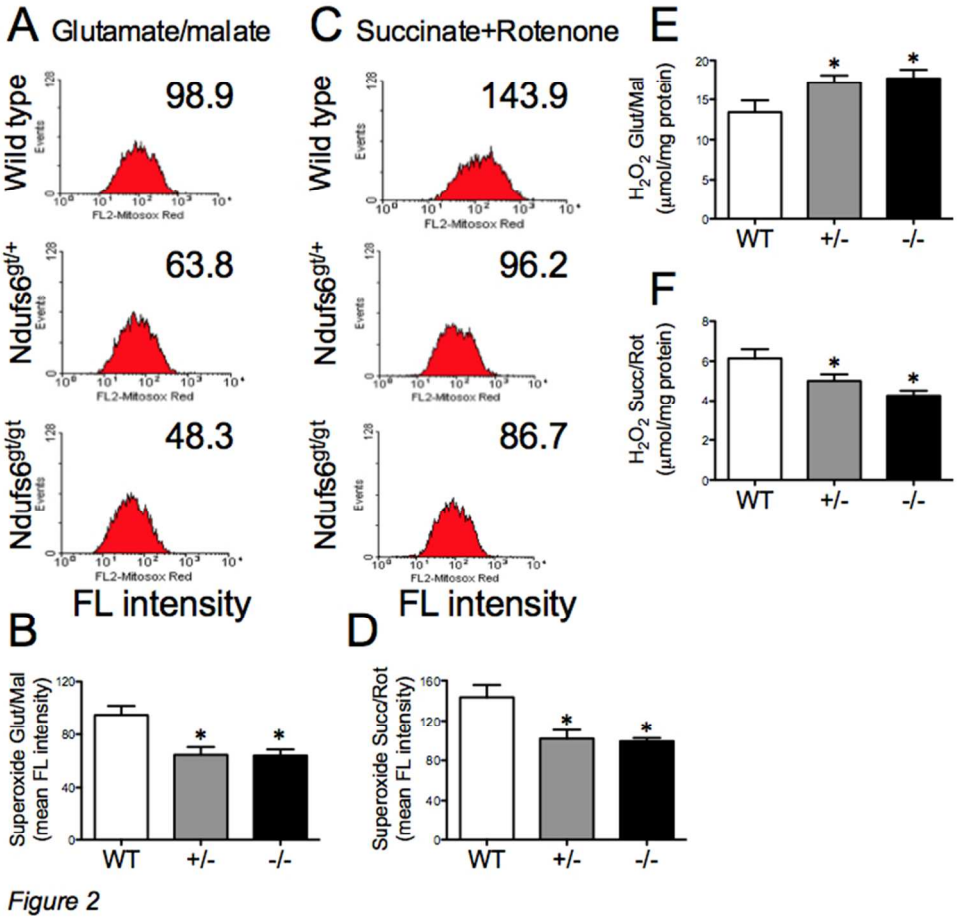

Figure 2

Renal mitochondrial reactive oxygen species generation. Renal cortical mitochondria from WT, Ndufs6gt/+mice and Ndufs6gt/gt mice were assayed for superoxide production using the MitoSox Red dye in the presence of A-B 10 mM glutamate and 10 mM malate, or C-D 10 mM succinate and 2.5 µM rotenone. Samples were analysed by flow cytometry using excitation at 400 nm with detection at 590 nm in the FL2 channel. Representative histograms showing mean intensity of MitoSOX fluorescence are shown for glutamate/malate (A), and succinate/rotenone (C), with corresponding quantitation shown in B and D respectively. Renal cortical mitochondria were incubated with (E) glutamate/malate or (F) succinate and rotenone and H2O2 production was assessed using the Amplex red assay probe with fluorescence detection. WT wild type, +/- Ndufs6gt/+mice, -/- Ndufs6gt/gt mice. *p <0.05 vs WT mice, n=6-8 per group; n=5 per group.

196x189mm (100 x 100 DPI)

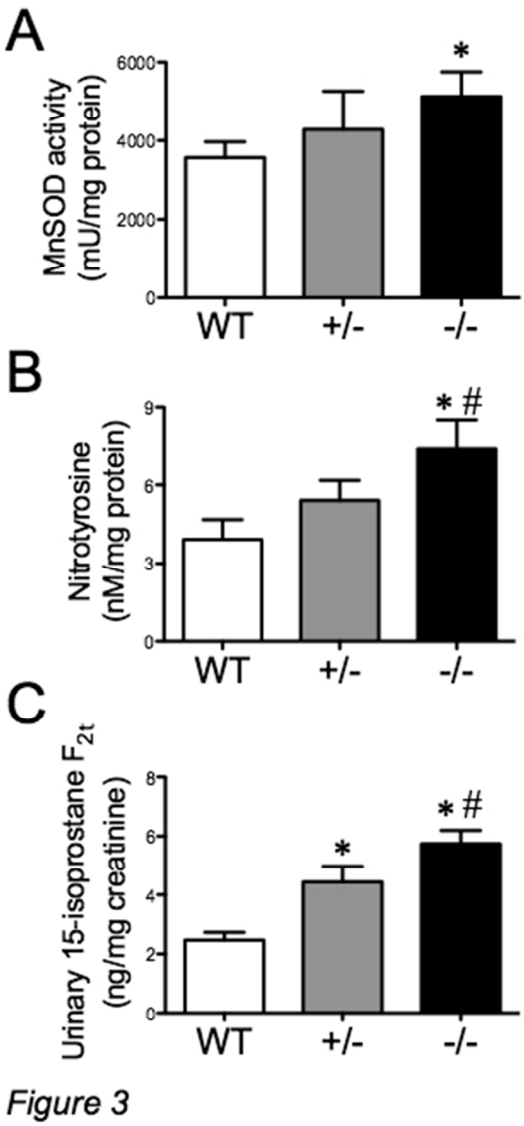

Figure 3

Figure 3: Manganese Superoxide Dismutase (MnSOD) activity and biomarkers of peroxynitrite damage and lipid peroxidation. Renal mitochondrial (A) MnSOD activity as measured by spectrophotometry, and (B) 3-nitrotyrosine content measured by enzyme-linked immunosorbent assay (ELISA). (C) Urinary 15-isoprostane F2t excretion as measured by ELISA. WT wild type, +/- Ndufs6gt/+mice, -/- Ndufs6gt/gt mice. *p<0.05 vs WT mice; #p<0.05 vs Ndufs6+/- mice; n=8 per group.
99x178mm (100 x 100 DPI)

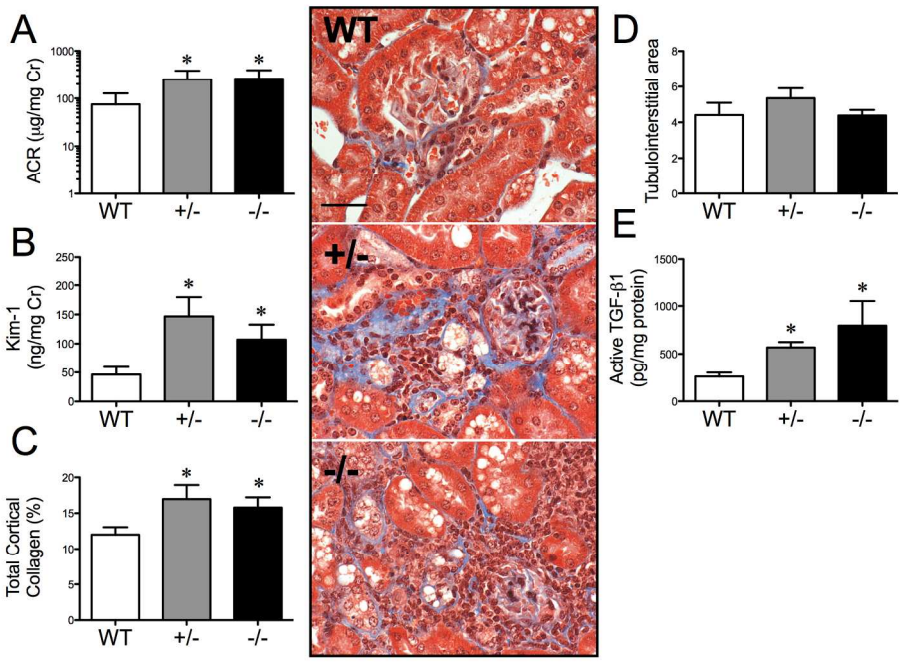

Figure 4

Renal phenotype.
(A) Urinary albumin to creatinine ratio (ACR) (data are geomean plus tolerance factor), (B) Urinary excretion of Kim-1, (C) Quantitation of total cortical collagen determined using Image ProPlus and representative photomicrographs of Masson's trichrome-stained sections of renal cortex from WT mice (top panel), Ndufs6+/- mice (middle panel) and Ndufs6-/- (bottom panel) mice showing collagen deposition in blue (x400 magnification, scale bar is equal to 25 µm). (D) Tubulointerstitial area evaluated by point counting technique. (E) Active TGF-β1 in renal cortical plasma membrane. WT wild type, +/- Ndufs6gt/+mice, -/- Ndufs6gt/gt mice. *p <0.05 vs WT mice; #p <0.05 vs Ndufs6+/- mice; n=8 per group.

198x151mm (300 x 300 DPI)

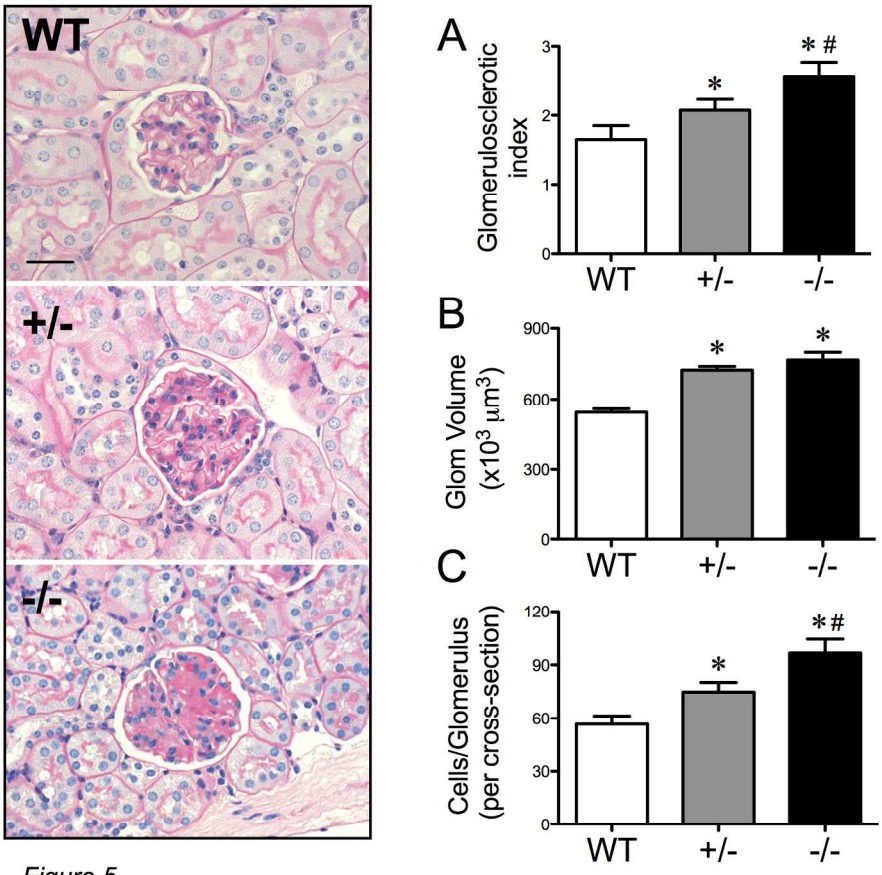

Figure 5

Glomerular injury. Representative photomicrographs of Periodic Acid Schiff (PAS) stained renal sections (x400 magnification, scale bar is equal to 25 µm) from WT mice (top panel), Ndufs6+/- mice (middle panel) and Ndufs6-/- mice (bottom panel), with (A) corresponding semiquantitative analysis of glomerulosclerosis. (B) Glomerular volume and (C) Cells/per glomerulus were assessed histologically as described in materials and methods. WT wild type, +/- Ndufs6gt/+mice, -/- Ndufs6gt/gt mice. *p <0.05 vs WT mice; #p <0.05 vs Ndufs6+/- mice; n=8 per group.
193x181mm (300 x 300 DPI)

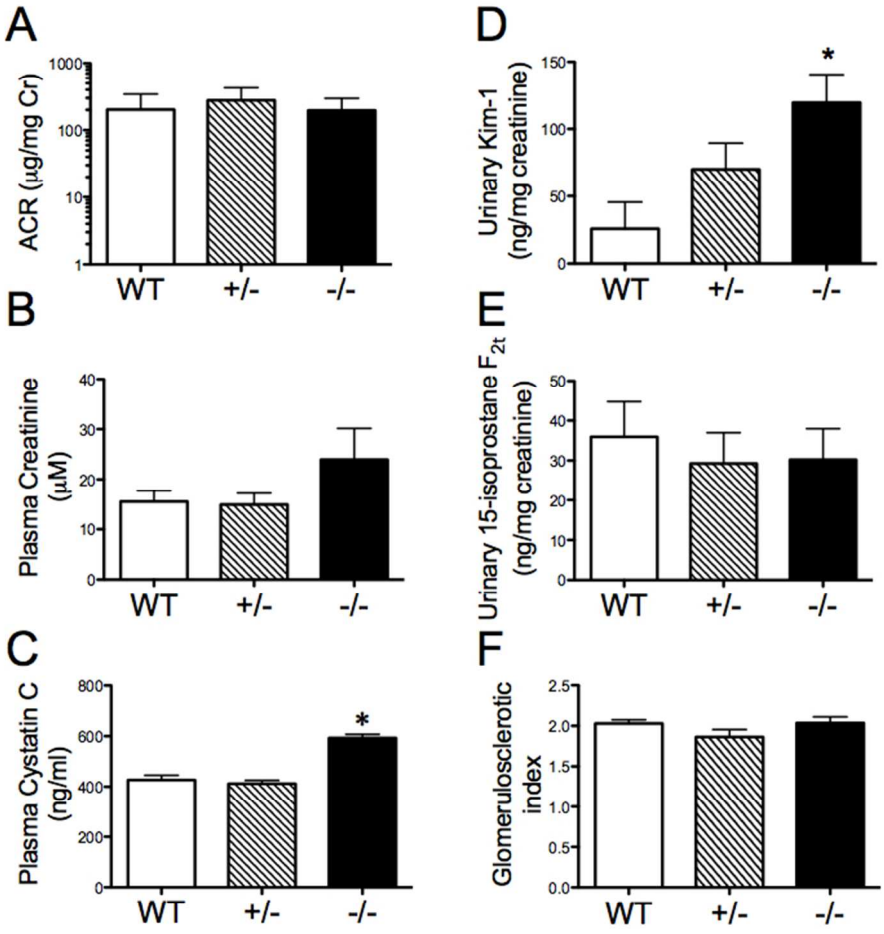

Figure 6

Figure 6: Renal phenotype of juvenile mice.
Urine, plasma and renal cortices were collected from 16 day old wild type, Ndufs6gt/+ and Ndufs6gt/gt mice and renal phenotype was determined. (A) Urinary albumin to creatinine ratio (ACR) (data are geomean plus tolerance factor), (B) Plasma creatinine as measured by high performance liquid chromatography, (C) Plasma cystatin C as measured by enzyme-linked immunosorbent assay (ELISA), (D) Urinary excretion of Kim-1 as determined by ELISA, (E) Urinary 15-isoprostane F2t excretion as measured by ELISA and (F) Semiquantitative analysis of glomerulosclerosis. WT wild type, +/- Ndufs6gt/+mice, -/- Ndufs6gt/gt mice. *p<0.05 vs WT mice; #p<0.05 vs Ndufs6+/- mice; n=3-5 mice per group.

196x202mm (100 x 100 DPI)